pH Dependence of Photolysis Intermediates in the Photoactivation of Rhodopsin Mutant E113Q†

James W. Lewis,‡ Istvan Szundi,‡ Wing-Yee Fu,§ Thomas P. Sakmar,§ and David S. Kliger*,‡

Department of Chemistry and Biochemistry, University of California, Santa Cruz, Santa Cruz, California 95064, and Howard Hughes Medical Institute and Laboratory of Molecular Biology and Biochemistry, Rockefeller University, 1230 York Avenue, New York, New York 10021

Received August 9, 1999; Revised Manuscript Received November 2, 1999

ABSTRACT: Glutamic acid at position 113 in bovine rhodopsin ionizes to form the counterion to the protonated Schiff base (PSB), which links the 11-*cis*-retinylidene chromophore to opsin. Photoactivation of rhodopsin requires both Schiff base deprotonation and neutralization of Glu-113. To better understand the role of electrostatic interactions in receptor photoactivation, absorbance difference spectra were collected at time delays from 30 ns to 690 ms after photolysis of rhodopsin mutant E113Q solubilized in dodecyl maltoside at different pH values at 20 °C. The PSB form (pH 5.5, $\lambda_{max} = 496$ nm) and the unprotonated Schiff base form (pH 8.2, $\lambda_{max} = 384$ nm) of E113Q rhodopsin were excited using 477 nm or 355 nm light, respectively. Early photointermediates of both forms of E113Q were qualitatively similar to those of wild-type rhodopsin. In particular, early photoproducts with spectral shifts to longer wavelengths analogous to wild-type bathorhodopsin were seen. In the case of the basic form of E113Q, the absorption maximum of this intermediate was at 408 nm. These results suggest that steric interaction between the retinylidene chromophore and opsin, rather than charge separation, plays the dominant role in energy storage in bathorhodopsin. After lumirhodopsin, instead of deprotonating to form metarhodopsin I_{380} on the submillisecond time scale as is the case for wild type, the acidic form of E113Q produced metarhodopsin I_{480}, which decayed very slowly (exponential lifetime = 12 ms). These results show that Glu-113 must be present for efficient deprotonation of the Schiff base and rapid visual transduction in vertebrate visual pigments.

To establish a stable pair of opposite charges within the low dielectric constant interior of a transmembrane protein requires considerable energy. Thus, where one exists, as it does in the active site of the visual pigment rhodopsin, it presumably has a key role in one or more aspects of function. Two general motifs seem to exist in the Schiff base−opsin interaction in visual pigments depending on a primary phylogenetic division. At the position where vertebrate visual pigments have an ionizable side chain, invertebrate visual pigments have an aromatic residue which remains neutral (*1, 2*). This difference likely accounts for some of the variations in the early photointermediates in the activation pathways of vertebrate versus invertebrate visual pigments. A useful approach to understand how electrostatic interactions participate in rhodopsin function is to express mutants with replacements of charged residues and then characterize the resultant pigments with fast optical absorbance measurements, which can resolve many steps in the functional chain of activation. Such measurements are possible using a microscale technique to obtain kinetic spectra using small amounts of pigment available from heterologous expression systems (*3*).

Site-directed mutagenesis of bovine rhodopsin has shown that Glu-113 provides the counterion to the PSB[1] formed between 11-*cis*-retinal and Lys-296 (*4*−*6*). One important reason to evolve a stable PSB is that it red-shifts the absorption spectrum of the retinal-based pigments to match the portion of the ambient solar spectrum useful for visual photosensitivity. Tuning the absorbance maxima to produce pigments with overlapping spectra for color discrimination is accomplished using other polar and polarizable side chains (*7*). However, color regulation may not be the only reason for having an ionizable group at position 113, since in all cases where the sequence of a vertebrate ultraviolet-sensitive pigment is known, glutamic acid remains in the analogous position (*8, 9*). Distinct from its possible counterion function, another role for an ionizable residue in that position is in the shut off of signaling. Mutants with neutral groups at position 113 have been shown to display constituitive activity (i.e., to activate transducin in the absence of chromophore) (*10, 11*). This is consistent with the observation that Glu-113 protonates in the metarhodopsin II (meta II) photointermediate (*12*), suggesting a central role for that residue in

† This work was supported by Grant EY00983 (to D.S.K.) from the National Eye Institute of the National Institutes of Health and the Allene Reuss Memorial Trust. T.P.S. is an Associate Investigator of the Howard Hughes Medical Institute.

‡ University of California, Santa Cruz.

§ Howard Hughes Medical Institute, Laboratory of Molecular Biology and Biochemistry, Rockefeller University.

[1] Abbreviations: batho, bathorhodopsin; BSI, blue-shifted intermediate; lumi, lumirhodopsin; MES, 2-(*N*-morpholino)ethanesulfonic acid; meta, metarhodopsin; PSB, protonated Schiff base; TRIS, tris(hydroxymethyl)aminomethane; WT, wild type.

10.1021/bi991860z CCC: $19.00
Published on Web 12/23/1999

the activation mechanism. Previous work has shown that mutation of Glu-113 to a neutral residue does not prevent the formation of a PSB, since at low pH an anion can be recruited from the solution to serve as counterion (*5*, *6*). This property of Glu-113 mutants such as E113Q allows the study of the activation mechanism of either protonated or unprotonated Schiff base forms depending on the initial pH.

We report here the measurement of absorbance difference spectra of the basic (UV-absorbing) and acidic (visible-absorbing) forms of rhodopsin mutant E113Q. The E113Q replacement was chosen since the glutamic acid to glutamine amino acid substitution is isosteric, while removing a potential negative charge. The controlled comparison of the early photolysis intermediates of the protonated and unprotonated Schiff base forms of mutant pigment E113Q provides insights into the role of electrostatic modifications of the chromophore-binding pocket in receptor photoactivation. Both forms of the E113Q pigment formed red-shifted bathorhodopsin-like early photoproducts that decayed to lumirhodopsin-like intermediates. However, the kinetics of later photoproducts were markedly affected by the removal of the Glu-113 counterion. The implications for the relative roles of steric and electrostatic chromophore−opsin interactions in the mechanism of receptor photoactivation are discussed.

MATERIALS AND METHODS

Preparation of Rhodopsin Mutants. Site-directed mutagenesis of bovine opsin was carried out as previously reported (*5*). Opsin genes were expressed in COS-1 cells, and the product protein was regenerated with 11-*cis*-retinal. The resulting pigment was purified and concentrated as described previously (*13*, *14*). For the pH 5.5 measurements, the final buffer composition was 25 mM MES, 30 mM NaCl, 60 mM KCl, and 2 mM $MgCl_2$ with 0.1% (w/v) dodecyl maltoside. At pH 8.2, the same solution composition was used except that TRIS was the pH buffer instead of MES.

Time-Resolved Spectroscopy. Individual 1 μL samples were photolyzed by 7 ns (fwhm) laser pulses. The change in the absorption spectrum at a particular time delay after photolysis, ranging from 30 ns to 690 ms, was measured using a gated optical multichannel analyzer (*3*). For pH 5.5 measurements, the samples were excited using 477 nm light from a dye laser pumped by the 355 nm third harmonic of a Nd:YAG laser. For excitation of the unprotonated Schiff base chromophore of samples at pH 8.2, the 355 nm third harmonic pulses were used directly. In both cases, the energy delivered to the sample was 80 μJ/mm^2. Absorbance changes were monitored using a flashlamp producing white probe light that was polarized at 54.7° relative to the laser polarization direction in order to minimize kinetic artifacts due to rotational diffusion. The path length of the probe light in the sample was 2 mm, and the sample temperature was maintained at 20 °C.

Fresh sample was pumped into the optical path from a computer-controlled syringe after each photolysis pulse. Photolyzed sample flowed out of the optical path into the volume above an L-shaped plastic insert, which forms the flow channel in the cuvette (*3*). Since a laser pulse typically bleaches only ~30% of a wild-type (WT) rhodopsin sample, and black surfaces in the flow channel reduce photolysis by succeeding laser pulses, approximately 50% of the pigment remains unbleached after the initial photolysis run has been completed. In the case of rhodopsin mutants, the remaining pigment can provide useful information, particularly if the initial pigment absorbance was high, as was the case for some samples used here (up to 0.73 AU/cm). In such cases, after assessment of the remaining pigment using conventional UV/Vis spectrophotometry, a second series of photolysis measurements was conducted using that material. Care must be taken interpreting rephotolysis data because of the possible production of stable photoproducts during the initial photolysis. However, for that very reason, rephotolysis data can be useful for detecting the formation of isopigments (9-*cis*-retinal chromophore).

Data Analysis. The set of experimental difference spectra, $\{\Delta A(\lambda,t)\}$, were fit as described previously (*15*) to a function whose form was a sum of exponential decays:

$$\Delta a(\lambda,t) \equiv b_0(\lambda) + b_1(\lambda)\exp(-t/\tau_1) + b_2(\lambda)\exp(-t/\tau_2) + \ldots$$

The apparent lifetimes, τ_i, and the difference spectra, or b-spectra, $b_i(\lambda)$, associated with the individual lifetimes are unambiguously determined by the fitting process. If one photointermediate completely transforms into another in an exponential process, and it is well isolated in time from other processes, then the b-spectrum associated with the isolated process can be simply interpreted as the difference between the spectra of the two intermediates. However, in general, a b-spectrum must be decomposed into multiple intermediate spectra consistent with the prevailing mechanism (which must be determined). A procedure for finding the mechanism and determining spectra of photointermediates has been described previously (*16*). That method was extended somewhat in the present work because the limited number of delay times used here introduced significant uncertainty in some of the lifetimes, which produced similar uncertainty in the associated b-spectra. While the original method was useful for determining what reaction scheme generally fit the data, with a small number of experimental difference spectra the best fit to the chosen mechanism resulted from directly fitting the data using the model intermediate spectra. The results of both methods were qualitatively similar, but better fits were obtained with the latter method for the data obtained here from the limited amounts of E113Q rhodopsin mutant available.

RESULTS

E113Q Rhodopsin Photolysis at pH 5.5. Rhodopsin mutant pigment E113Q exists in a pH-dependent equilibrium of two spectral forms (Figure 1). Absorbance difference spectra were collected at a series of delays following 477 nm excitation of the E113Q rhodopsin mutant in detergent solution at pH 5.5 (Figure 2, top). The increased absorbance seen in the 560 nm region at 30 ns and its subsequent decay, during the first microsecond after excitation, are hallmarks of the bathorhodopsin (batho) intermediate seen after WT rhodopsin photolysis. As was the case for WT rhodopsin, the pH 5.5 E113Q rhodopsin difference spectra were best fit by two exponential processes in the time range where batho decay occurs. The lifetimes determined were 40 ns and 1.1 μs, and

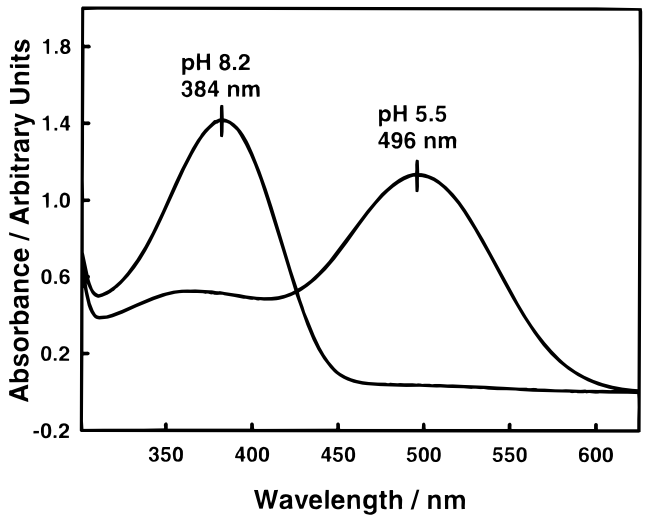

FIGURE 1: UV−visible absorption spectra of rhodopsin mutant E113Q at pH 5.5 and 8.2. The mutant pigment was purified in dodecyl maltoside solution from COS cells. The λ_{max} values for the two spectral forms of the pigment were 384 and 496 nm under the conditions used for the photolysis experiments.

the corresponding b-spectra are shown in the lower panel of Figure 2. At early times after photolysis, the only qualitative difference from what is observed for WT rhodopsin is the absence of the usual shallow negative absorbance band from 400 to 500 nm. WT rhodopsin absorbs more strongly than its photoproducts in that spectral region during the first ~120 ns after photolysis, which is not the case for E113Q rhodopsin.

The results for later delay times after photolysis of E113Q rhodopsin show more significant qualitative differences from WT rhodopsin. Photolysis of detergent solutions of WT rhodopsin near room temperature yields photoproducts whose absorbance maxima monotonically blue-shift with time. In contrast, the maximum in the absorbance difference spectrum of E113Q rhodopsin at pH 5.5 shifts toward the red from 1 μs to 1 ms. This shift was evident in all experiments including one where the signal was smaller because the pigment concentration was less than one-third that of the sample which produced the data shown in Figure 2. After 1 ms, the red shift reverses, and a ~380 nm absorbing product is observed. This final process is much slower than the comparable process occurring in detergent solutions of WT rhodopsin, which is 90% complete within 1 ms. Since the spectral shift observed from 1 μs to 1 ms is in the opposite direction from that after 1 ms, two distinct processes must be involved. These were fit to exponential lifetimes of 540 μs and 11 ms, associated with b_3 and b_4, respectively (Figure 2, bottom). The precision in the determination of τ_3 was not as high as for the other apparent lifetimes because of the distribution of the experimental delay times, but the associated b-spectrum, b_3, is relatively unaffected by that uncertainty.

The absence of negative absorbance changes in the 30 ns data noted above might result from formation of a small amount of E113Q isorhodopsin by photolysis of E113Q batho. Because isopigments typically are blue-shifted and have higher extinction coefficients relative to 11-cis pigments, their formation tends to fill in the bleaching region below 500 nm. This change is prompt and persistent because

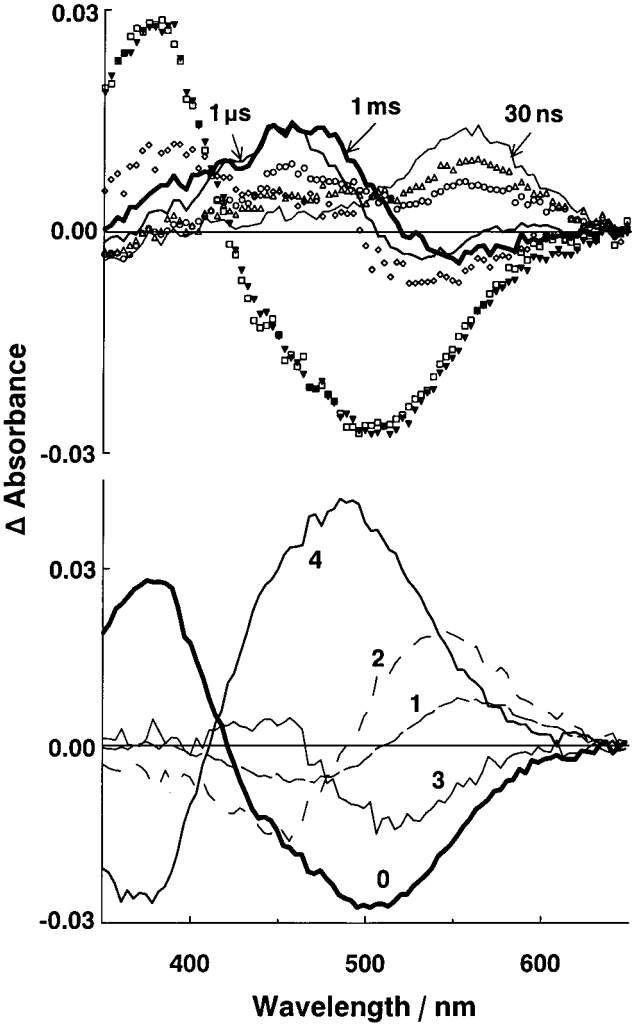

FIGURE 2: Absorbance changes occurring after 477 nm photolysis of E113Q rhodopsin at pH 5.5. (Top) Difference spectra were collected 30, 90, and 230 ns; 1 μs; and 1, 5, 50, and 690 ms after the 7 ns photolysis pulse. The sample used to collect these data consisted of 450 μL of a 0.1% (w/v) dodecyl maltoside solution whose absorbance at 496 nm was 0.140 in the 0.2 cm path length of the apparatus. The heavy line shows the 1 ms difference spectrum which is the only spectrum in the series which reverses the general trend of blue-shifting absorbance with increasing delay time after photolysis. Curves are as labeled or 90 ns (△), 230 ns (○), 5 ms (◇), 50 ms (▼), and 690 ms (□). (Bottom) The b-spectra were determined from fitting the data shown in the top panel. The curves labeled 1−4 correspond to apparent lifetimes of 52 ns, 992 ns, 532 μs, and 12 ms, respectively. The curve labeled 0 represents the infinite time difference spectrum.

9-cis pigments are usually stable, but is most evident at early times when only a shallow bleaching region normally appears. The formation of isopigment during initial photolysis can be detected by comparison of the bleaching region of rephotolysis data at a suitably long time delay with similar data from the initial photolysis run. Isopigment formation will slightly red-shift the bleaching region of the initial photolysis data because the net difference spectrum for 11-cis to 9-cis conversion is negative above ~500 nm and positive below. An opposite distortion will occur in the bleaching region of rephotolysis data because there the primary error comes from photolysis of the blue-shifted 9-cis pigment produced in the initial photolysis. As shown in Figure 3, the bleaching region of the 50 ms rephotolysis trace is deeper and slightly blue-shifted compared with the initial

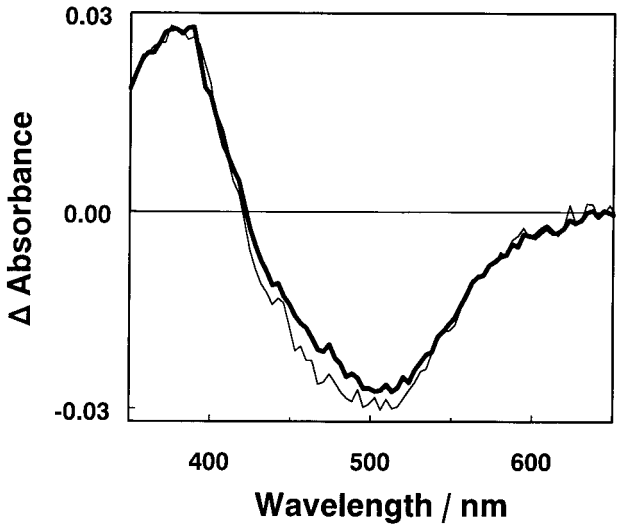

FIGURE 3: Comparison of initial and rephotolysis difference spectra 50 ms after 477 nm excitation of E113Q rhodopsin at pH 5.5. After completion of the initial photolysis run, UV/Vis spectrophotometry showed that the sample used to collect the data shown in Figure 2 contained substantial amounts of unphotolyzed pigment. The sample was reloaded into the syringe pump, and a second set of photolysis measurements was conducted, concentrating primarily on the later delay times. Following this, a third run was conducted. Shown here is the absorbance difference spectrum collected at 50 ms delay in the initial run (heavy line) compared to the average of the 50 ms spectra collected in the two rephotolysis runs (light line) scaled to have the same amplitude near 380 nm as the initial photolysis data. Both of the individual rephotolysis difference spectra had the same qualitative differences from the initial photolysis data as the averaged spectrum shown here, but because signals were smaller in the rephotolysis data the signal-to-noise ratios in the individual spectra were lower.

Scheme 1

$$\text{batho} \underset{k_2}{\overset{k_1}{\rightleftharpoons}} \text{BSI} \xrightarrow{k_3} \text{lumi} \xrightarrow{k_4} \text{meta I}_{480} \xrightarrow{k_5} \text{meta II}$$

Table 1: Rate Constants for E113Q Rhodopsin Photolysis

	rate (s^{-1})				
	k_1	k_2	k_3	k_4	k_5
E113Q rhodopsin, pH 5.5	1.05×10^7	1.33×10^7	2.12×10^6	1.85×10^3	94.1
E113Q rhodopsin, pH 8.2	1.08×10^7	1.39×10^7	2.65×10^6	9.88×10^4	37.5
WT (COS cell)[a]	1.0×10^7	5.3×10^6	5.3×10^6	*b*	3200

[a] Reference *18*. [b] Not observed in this preparation.

photolysis data, as would be expected if some E113Q isorhodopsin were formed during the initial photolysis run by secondary photolysis of E113Q batho.

The data for E113Q rhodopsin at pH 5.5 (Figure 2, top) can be fit to a scheme (Scheme 1) similar to that obeyed after photolysis of WT rhodopsin under similar conditions). The rate constants obtained are shown in Table 1, and the λ_{max} values of the intermediates determined from fitting are shown in Table 2. Figure 4 shows the level of agreement between the model intermediate spectra and the experimentally determined spectra. These results have been corrected for 10% conversion of the initial photoproduct into E113Q isorhodopsin.

E113Q Rhodopsin Photolysis at pH 8.2. The top panel of Figure 5 shows absorbance difference spectra collected after

Table 2: Absorption Maxima for E113Q Rhodopsin Photolysis Intermediates

	λ_{max} (nm)				
	batho	BSI	lumi	meta I	meta II
E113Q rhodopsin, pH 5.5	530	483	470	488	378
E113Q rhodopsin, pH 8.2	408	377	370	375	377
WT (COS cell)[a]	531	479	490	*b*	380

[a] Reference *18*. [b] Not observed in this preparation.

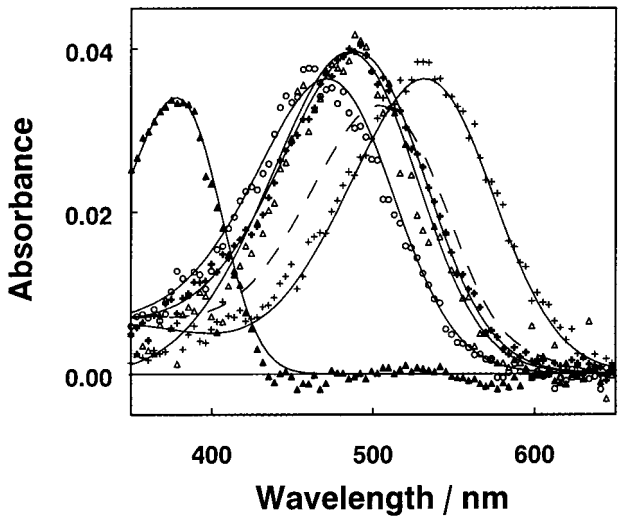

FIGURE 4: Spectra of intermediates appearing after photolysis of E113Q rhodopsin at pH 5.5. The smooth curves show the spectra of the model intermediates, and the symbols [batho (+), BSI (△), lumi (○), meta I_{480} (thick plus signs), meta II (▲)] show the result obtained using the rate constants shown in Table 1. The dashed curve shows the spectrum of the pigment photolyzed to produce each of the intermediates shown. This pigment spectrum, being derived from the photolysis data, is subject to experimental uncertainties. These include the need to estimate the amount of isopigment formed during photolysis (see text) as well as the noise inherent in the data.

355 nm photolysis of an E113Q rhodopsin sample at pH 8.2. Positive absorbance peaking near 440 nm is seen 30 ns after photolysis with subsequent decay. This early red-shifted photoproduct is similar to WT bathorhodopsin when allowance is made for the ~120 nm blue shift induced by deprotonation of the chromophore at pH 8.2. Direct fitting of the data yielded a single exponential on the submicrosecond time scale with a lifetime of 290 ns. However, the single-exponential fit cannot necessarily be construed as indicating that the usual two processes are absent since the signal amplitude was smaller and more compressed in wavelength range at pH 8.2 compared with that at pH 5.5, making the signal-to-noise ratio lower at pH 8.2 (see below).

The b-spectrum associated with the 290 ns process is shown as b_1 in the lower panel of Figure 5. From 1 μs to 1 ms after photolysis, a shift to longer wavelength absorption was seen followed by a final, slow red shift. These late processes were fit with lifetimes of 7 μs and 40 ms, but there is uncertainty in both lifetimes because the spectral shifts for both processes were small. Despite this, the changes observed were reproducible in repeated experiments, and the b-spectra, which are again less uncertain than the lifetimes, are shown in the lower panel of Figure 5.

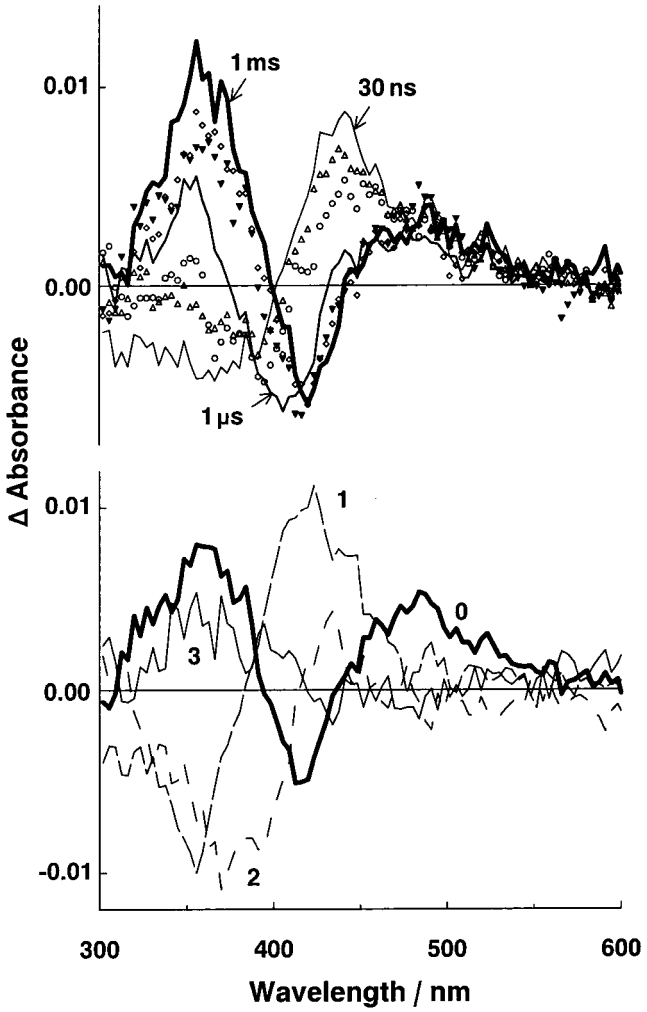

FIGURE 5: Absorbance changes occurring after 355 nm photolysis of E113Q rhodopsin at pH 8.2. (Top) Difference spectra were collected 30, 90, and 230 ns; 1 μs; and 1, 50, and 690 ms after the 7 ns photolysis pulse. The sample used to collect these data consisted of 450 μL of a 0.1% (w/v) dodecyl maltoside solution whose absorbance at 384 nm was 0.146 in the 0.2 cm path length of the apparatus. Curves are as labeled or 90 ns (△), 230 ns (○), 50 ms (◇), and 690 ms (▼). (Bottom) The b-spectra were determined from fitting the data shown in the top panel. The curves labeled 1−3 correspond to apparent lifetimes of 290 ns, 7 μs, and 40 ms, respectively. The curve labeled 0 represents the infinite time difference spectrum.

At longer wavelengths, beyond the region where the decay of the batho-like product occurs, the data in the top panel of Figure 5 show additional tails of positive absorbance. The stability of the absorption even during the formation of 380 nm absorbing products suggests the formation of a small amount of stable photoproduct containing a PSB. A possible explanation, which parallels events in the sample at pH 5.5, is that E113Q isorhodopsin forms and the visible absorption arises from the Schiff base pK_a of the iso form being somewhat higher than that of the 11-cis form. However, direct experimental measurements of the pK_a's of E113Q regenerated with 11-*cis*- or 9-*cis*-retinal displayed statistically identical values of 6.05 ± 0.08 and 5.99 ± 0.16, respectively (data not shown). An alternative explanation of the tails at late times is formation of a trace of meta I_{480}. High pH favors meta I_{480} in the WT meta I_{480} ⇄ meta II equilibrium; however, that is only the case in membrane or digitonin solution. No pH-dependent meta I_{480} ⇄ meta II equilibrium exists for dodecyl maltoside solutions of WT rhodopsin. Whatever the origin of the tails, since they have small amplitude compared with the maximum signal size and have little or no time dependence, it is clear that they come from minor participants in the kinetic processes. Therefore, whether they originate in protonated E113Q meta I_{480} or in some other species, they will not significantly affect the characterization of the main intermediates.

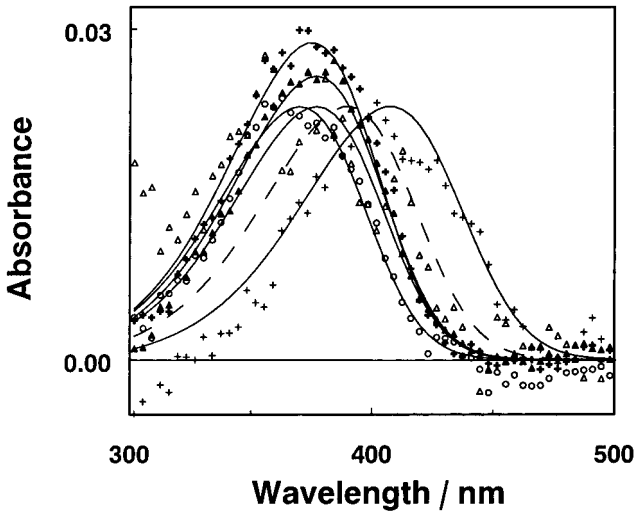

FIGURE 6: Spectra of intermediates appearing after photolysis of E113Q rhodopsin at pH 8.2. The smooth curves show the spectra of the model intermediates, and the symbols [batho (+), BSI (△), lumi (○), meta I_{380} (thick plus signs), meta II (▲)] show the result obtained using the rate constants from Table 1. The dashed curve shows the spectrum of the pigment photolyzed to produce each of the intermediates.

After photolysis at pH 8.2, E113Q rhodopsin, which contains an unprotonated Schiff base chromophore at this pH (*17*), forms a red-shifted bathorhodopsin-like photoproduct. While the data up to 1 μs in the top panel of Figure 5 only have a signal-to-noise ratio high enough to allow fitting of a single exponential, there is a high probability that two processes underlie the progression after photolysis. For all previous mutants or artificial pigments where similar amounts of batho-like absorbance appeared, two sub-microsecond processes were resolvable when high enough signal-to-noise was achieved, as was the case above for E113Q rhodopsin at pH 5.5. Further, examination of the spectra of the intermediates obtained from fitting a straight sequential scheme to the b-spectra from the three-exponential fit gave a first intermediate with an unusually broad spectral shape. A similar, unusually broad first intermediate spectrum results when WT or E113Q rhodopsin at pH 5.5 are fit with fewer than the required number of exponentials. To determine whether the pH 8.2 data could be fit with a similar set of intermediates used to fit the pH 5.5 data, the intermediates used to fit E113Q rhodopsin at pH 5.5 (except for meta II) were shifted to higher energy by the same amount as the shift of the pigment spectrum on Schiff base deprotonation. These blue-shifted intermediates were then used to directly fit the pH 8.2 data. A reasonable fit was obtained, which was slightly improved by minor adjustments to the intermediate spectra, as shown in Table 2. The rate constants deduced from the fit are given in Table 1. Figure 6 shows the level of agreement between the model intermediate spectra and the experimentally determined spectra.

Scheme 2

$$\text{batho}^{*} \underset{k_2}{\overset{k_1}{\rightleftharpoons}} \text{BSI}^{*} \xrightarrow{k_3} \text{lumi}^{*} \xrightarrow{k_4} \text{meta I}_{380} \xrightarrow{k_5} \text{meta II}$$

The result of the fit shows that the scheme followed by E113Q rhodopsin after photolysis at pH 8.2 corresponds with that seen at pH 5.5 (Scheme 2).

Here, because the pigment has an unprotonated Schiff base, the early intermediates up to lumi are likely to as well (denoted by asterisk), and instead of meta I_{480} seen at pH 5.5, meta I_{380} assumes its usual place in the intermediate sequence of a detergent-solubilized sample. The final product can be identified as meta II because previous studies have shown that activation of the high-pH form with UV light produces a receptor which activates transducin (*13*).

DISCUSSION

The quantity of expressed pigment in samples available from heterologous expression systems is limited. Although detailed photolysis studies of mutant rhodopsins have been reported (*18*, *19*), it remains important to focus the scope of experiments since a complete characterization of photoproduct intermediates and kinetics is generally not yet routinely possible. The signal-to-noise ratio achieved in absorbance difference measurements and the range of times that can be studied are restricted. Our primary goal was to study the effect of the E113Q mutation in rhodopsin on early photoproducts, which typically display large spectral shifts, to better understand the influence of electrostatic effects on intermediate spectra. Characterization of late intermediate kinetics was a secondary goal. Preliminary measurements showed that significant absorbance changes were occurring on the sub-microsecond time scale after E113Q rhodopsin photolysis at pH 5.5. Therefore, the majority of absorbance measurements were made at delay times within that range. Fewer absorbance measurements were made at longer times, and characterization of the later reactions (following lumi decay) was less complete. By restricting the number of delay times, more averaging could be performed at the specific delays chosen and the accuracy of the difference spectra could be determined from their reproducibility.

Photolysis of E113Q rhodopsin produced a photointermediate analogous to the bathorhodopsin formed upon photolysis of WT rhodopsin. At both pH 5.5 and pH 8.2, the red shift (in cm^{-1}) in the absorption maximum of the E113Q bathorhodopsin relative to that of the unphotolyzed pigment was comparable within experimental uncertainty to what is observed for WT rhodopsin (see Table 2). Further, as reflected by the rate constants, the mutation did not destabilize the bathorhodopsin as is often the case for rhodopsin analogues made with synthetic retinal chromophores (*20*), and was also seen for rhodopsin mutants where the carboxylate counterion was moved to a different position (*18*). The results reported here unambiguously point to steric effects between the retinylidene chromophore and its protein pocket playing the dominant role in bathorhodopsin stability, with relatively minor tuning of that stability resulting from the electrostatic interaction between the PSB and counterion. A similar conclusion was suggested based on solid-state NMR spectroscopy and semiempirical quantum calculations that led to a model of bathorhodopsin in which the distance between the Schiff base and Glu-113 was similar to that in rhodopsin (*21*).

The E113Q photolysis results also contribute to understanding how PSB−counterion interactions contribute to the λ_{max} shifts of the photointermediates. Clearly, electrostatics, in the form of PSB−counterion interactions, and steric effects, mainly through bond torsions, both affect intermediate spectra. The blue shift of E113Q lumirhodopsin at both pH values, compared with WT lumirhodopsin, indicates that the presence of the Glu-113 counterion acts to red shift the lumi spectrum. This red shifting electrostatic effect in lumi partially reverses a steady blue shift, which would otherwise occur continuously through the batho → BSI → lumi sequence, presumably due to relaxing chromophore torsion. Significant pH-dependent differences were also observed in the sequence of the later intermediates that appeared after lumirhodopsin. While these changes depend on the protonation state of the retinylidene Schiff base, it is much more difficult to isolate an electrostatic role in the late intermediate reactions because late processes involve one or more protonation/deprotonation steps, fundamentally defeating straightforward analysis in electrostatic terms. Nevertheless, while proton transfer may interfere with a general energetic analysis, a specific sequence of protonation steps normally occurs in rhodopsin activation, and elucidation of the sequence and structure of the participating intermediates is a necessary step in understanding that process.

E113Q Rhodopsin at pH 5.5. While the same general scheme prevails for E113Q rhodopsin at pH 5.5 and for WT rhodopsin, some differences are evident. The equilibrium constant between batho and BSI seen here is slightly back-shifted ($K_{eq} = 0.82$) versus the forward-shifted WT rhodopsin value ($K_{eq} = 1.44$, *15*). Also, significant slowing of BSI decay to form lumi occurs, and when lumi does form, it is 22 nm more blue shifted compared to the value for WT.

A greater difference between E113Q rhodopsin at pH 5.5 and WT rhodopsin behavior occurs when lumi decays. Whereas deprotonation of the Schiff base occurs immediately with meta I_{380} formation for WT rhodopsin in detergent solution (*18*, *22*), for E113Q rhodopsin at pH 5.5, meta I_{480} forms instead and then deprotonates only very slowly to form a 380 nm absorber (here labeled meta II because it has been shown to activate transducin, *13*). The subsequent slow deprotonation of the Schiff base in E113Q rhodopsin at pH 5.5 is consistent with the observation in FTIR studies that the glutamate at position 113 becomes protonated at meta II (*12*). Thus, Glu-113 can be presumed to normally function as the Schiff base proton acceptor when meta I_{480} decays. However, in addition to supporting that conclusion of the FTIR results, the current work further shows that Glu-113 must also function as the Schiff base proton acceptor when meta I_{380} forms, since at pH 5.5 the E113Q mutation prevents the appearance of that intermediate as well. Given enough time (tens of milliseconds), the recruited chloride ion or some other group accepts the Schiff base proton from meta I_{480}, but even in a detergent sample where the branch to meta I_{380} is normally strongly favored, deprotonation to alternative sites is too slow to prevent essentially complete formation of the competing product, meta I_{480}.

Differences between E113Q rhodopsin at pH 5.5 and WT rhodopsin include an increase in the amount of E113Q isorhodopsin formed after 477 nm photolysis. This effect was

consistently seen in all experiments and cannot be explained by the presence of unusual amounts of blue-absorbing all-trans photointermediates forming during the laser pulse since the data show that less E113Q batho decay takes place during the 7 ns laser pulse than occurs after WT rhodopsin photolysis. Accumulation of E113Q isorhodopsin must result from either enhanced quantum yield for E113Q batho photolysis or diminished quantum yield for E113Q isorhodopsin photolysis compared with what occurs for WT rhodopsin. It should be noted that resonance Raman microprobe experiments also reported that the E113Q rhodopsin spectrum was dominated by 9-cis lines at 1150, 1205, and 1320 cm^{-1} (*17*, *23*). Given the large blue shift of E113Q lumi, it is interesting that enhancement of the E113Q isorhodopsin yield occurs since it has been shown that isopigments of both bovine rhodopsin and gecko P521 pigment produce lumi intermediates which are blue shifted relative to those which result from photolysis of the 11-cis pigments (*24*). The blue-shifted lumi in these cases presumably results from a distortion of the chromophore pocket induced by the 9-cis chromophore, which persists up to the lumi stage. It is thus possible that the blue shift of lumi seen here may result from a similar difference in the E113Q chromophore environment that reciprocally favors E113Q isorhodopsin formation.

E113Q Rhodopsin at pH 8.2. The results seen after 355 nm photolysis of the unprotonated Schiff base of E113Q rhodopsin show strong parallels with the behavior of the protonated form. The conclusion that batho*, BSI*, and lumi* continue to be unprotonated is based on the fact that their spectra are approximately 100 nm blue-shifted relative to the analogous pH 5.5 forms, consistent with their retaining the unprotonated Schiff base of the original pigment at pH 8.2. Even for the unprotonated form, a shift to longer wavelengths is seen initially at 30 ns. Decay of this early photoproduct up to lumirhodopsin follows a scheme which is analogous to what occurs for the protonated form of E113Q rhodopsin with all the intermediates shifted by the amount that the pigment spectrum itself shifts upon deprotonation. Again, batho* and BSI* intermediates have similar energetic shifts from the pigment spectrum compared with WT, and lumi* has more than twice the shift to shorter wavelengths. It should be noted that this conclusion concerning the large blue shift of lumi* follows directly from the b-spectrum, b_1, and does not depend on the extended direct fitting method used at pH 8.2 to determine the batho* and BSI* spectra. The fact that a continuing shift to shorter wavelengths occurs here for lumi*, in the absence of any possible change in PSB−counterion interaction, must indicate the presence of a sterically induced blue shift at the lumirhodopsin stage which in WT rhodopsin is partially counteracted by opposite changes in the PSB−counterion interaction.

Following lumi*, there is no unusual barrier to formation of meta I_{380} as appears in the pH 5.5 case, since at pH 8.2 the preexisting Schiff base deprotonation compensates for the absence of a proton acceptor at position 113. The unusual slowness of the final meta II formation step compared to what is normally seen for WT in detergent may be caused by the slowed proton uptake from solution at pH 8.2, since protonation of one or more non-Schiff base sites is known to be involved in meta II formation (*25*).

Role of the PSB in Visual Phototransduction. Glutamic acid 113 normally ionizes to form the counterion to the PSB in rhodopsin. The results obtained here show that mutation of Glu-113 to neutral glutamine has relatively little effect on the early intermediates which form and decay after photolysis. This result is consistent with conclusions of previous resonance Raman microprobe experiments for E113Q bathorhodopsin (*17*), confirming bathorhodopsin formation for both the protonated and unprotonated Schiff base forms in those experiments. While this may not be too remarkable for the low-pH form of E113Q rhodopsin which can recruit a chloride counterion from solution, it is quite surprising that the pH 8.2 form, which completely lacks the electrostatic, PSB−counterion interaction, behaves so normally at early times. It undergoes a decay sequence parallel to WT, differing principally in the static shift of the photointermediate absorbance maxima which originates from the ground-state absorbance spectrum of the unphotolyzed pigment. Much greater changes in the kinetics of bathorhodopsin decay are observed when the 13-methyl group is removed from the chromophore (*26*) or when the counterion is moved by one helix turn in the mutant E113A/A117E (*18*). These might at first seem to be less severe perturbations than the E113Q mutation.

A parallel exists between the behavior of E113Q at pH 8.2 seen here and that seen recently for the mouse UV pigment (*27*). While glutamic acid occurs at position 108 in the mouse UV pigment (analogous to Glu-113 in bovine rhodopsin), evidence exists for the chromophore being an unprotonated Schiff base. Similarly to what we observe for E113Q at 20 °C, photolysis of the mouse UV pigment produced a red-shifted batho which could be trapped at 70 K. Thus, it seems clear that a relatively normal batho intermediate can be formed from an uncharged binding site.

This picture of rhodopsin photoactivation where steric effects make the dominant contributions to the stability of the early photointermediates is consistent with the implications arising from a rhodopsin model proposed previously (*28*). With respect to the photostability of the early intermediates, Gln-113 acts to increase isorhodopsin formation, possibly implicating charge at that position interacting with the PSB to reduce isorhodopsin formation. This would, of course, not be important at the fluence levels where vision normally takes place, but it may indicate that a negative charge at 113 contributes to distortion of the chromophore away from the 9-cis configuration.

The enhancement of visual pigment sensitivity by Schiff base protonation has been discussed (*29*). From the measurements reported here, it is difficult to determine absolute quantum yields since optimizing the signal-to-noise in absorbance measurements necessitates relatively high fluence excitation. A relative value can be estimated by comparing the positive transient absorbance due to batho formation at the two pH values and making appropriate spectral and quantum flux corrections. Such a comparison (using $b_1 + b_2$ at pH 5.5 and b_1 alone at pH 8.2) indicates that the quantum yield for 355 nm photolysis of the pH 8.2 form is somewhat smaller than for 477 nm excitation of the pH 5.5 form, but that the difference is less than a factor of 2. The fact that no dramatic reduction in isomerization quantum yield occurs on deprotonation is consistent with previous results for transducin activation by E113Q rhodopsin (*13*)

and is also consistent with the occurrence in nature of UV-sensitive, invertebrate visual pigments whose sequences lack potential counterions, and hence are likely to function with the Schiff base deprotonated (*30*−*32*).

The most important role of Glu-113 in rhodopsin photoactivation seems to involve the late intermediates. It is apparently the obligatory acceptor of the Schiff base proton in both meta I_{380} and meta II formation. Even the E113D mutation significantly slowed Schiff base deprotonation (*18*), and a much greater slowing is seen with the E113Q mutation. Note that the 12 ms process seen here for pH 5.5 E113Q rhodopsin in detergent solution would likely become much slower in the native membrane environment, seriously degrading system response. In fact, the stability of PSB intermediates in the activation sequence of invertebrates may simply be due to the absence of a proton acceptor in the position analogous to 113. The data for k_4 suggest an even earlier dependence of the meta I formation rate on Schiff base deprotonation. While this seems a plausible mechanism, given the uncertainty in those rates the difference is not significant. A goal of future experiments is to examine changes in that reaction and the details of subsequent meta II formation with higher signal-to-noise measurements.

REFERENCES

1. Nakagawa, M., Iwasa, T., Kikkawa, S., Tsuda, M., and Ebrey, T. G. (1999) *Proc. Natl. Acad. Sci. U.S.A. 96*, 6189−6192.
2. Hashimoto, S., Takeuchi, H., Nakagawa, M., and Tsuda, M. (1996) *FEBS Lett. 398*, 239−242.
3. Lewis, J. W., and Kliger, D. S. (1993) *Rev. Sci. Instrum. 64*, 2828−2833.
4. Nathans, J. (1990) *Biochemistry 29*, 9746−9752.
5. Sakmar, T. P., Franke, R. R., and Khorana, H. G. (1989) *Proc. Natl. Acad. Sci. U.S.A. 86*, 8309−8313.
6. Zhukovsky, E. A., and Oprian, D. D. (1989) *Science 246*, 928−930.
7. Kochendoerfer, G. G., Lin, S. W., Sakmar, T. P., and Mathies, R. A. (1999) *Trends Biochem. Sci. 24*, 300−305.
8. Hisatomi, O., Satoh, T., Barthel, L. K., Stenkamp, D. L., Raymond, P. A., and Tokunaga, F. (1996) *Vision Res. 36*, 933−939.
9. Wilkie, S. E., Vissers, P. M. A. M., Das, D., DeGrip, W. J., Bowmaker, J. K., and Hunt, D. M. (1998) *Biochem. J. 330*, 541−547.
10. Cohen, G. B., Oprian, D. D., and Robinson, P. R. (1992) *Biochemistry 31*, 12592−12601.
11. Robinson, P. R., Cohen, G. B., Zhukovsky, E. A., and Oprian, D. D. (1992) *Neuron 9*, 719−725.
12. Jäger, F., Fahmy, K., Sakmar, T. P., and Siebert, F. (1994) *Biochemistry 33*, 10878−10882.
13. Fahmy, K., and Sakmar, T. P. (1993) *Biochemistry 32*, 9165−9171.
14. Zvyaga, T. A., Fahmy, K., and Sakmar, T. P. (1994) *Biochemistry 33*, 9753−9761.
15. Hug, S. J., Lewis, J. W., Einterz, C. M., Thorgeirsson, T. E., and Kliger, D. S. (1990) *Biochemistry 29*, 1475−1485.
16. Szundi, I., Lewis, J. W., and Kliger, D. S. (1997) *Biophys. J. 73*, 688−702.
17. Lin, S. W., Sakmar, T. P., Franke, R. R., Khorana, G. H., and Mathies, R. A. (1992) *Biochemistry 31*, 5105−5111.
18. Jäger, S., Lewis, J. W., Zvyaga, T. A., Szundi, I., Sakmar, T. P., and Kliger, D. S. (1997) *Biochemistry 36*, 1999−2009.
19. Jäger, S., Han, M., Lewis, J. W., Szundi, I., Sakmar, T. P., and Kliger, D. S. (1997) *Biochemistry 36*, 11804−11810.
20. Randall, C. E., Lewis, J. W., Hug, S. J., Björling, S. C., Eisner-Shanas, I., Friedman, N., Ottolenghi, M., Sheves, M., and Kliger, D. S. (1991) *J. Am. Chem. Soc. 113*, 3473−3485.
21. Han, M., and Smith, S. O. (1995) *Biochemistry 34*, 1425−1432.
22. Mah, T. L., Szundi, I., Lewis, J. W., Jäger, S., and Kliger, D. S. (1997) *Photochem. Photobiol. 68*, 762−770.
23. Palings, I., Pardoen, J. A., van den Berg, E., Winkel, C., Lugtenburg, J., and Mathies, R. A. (1987) *Biochemistry 26*, 2544−2556.
24. Lewis, J. W., Liang, J., Ebrey, T. G., Sheves, M., Livnah, N., Kuwata, O., Jäger, S., and Kliger, D. S. (1997) *Biochemistry 36*, 14593−14600.
25. Arnis, S., and Hofmann, K. P. (1993) *Proc. Natl. Acad. Sci. U.S.A. 90*, 7849−7853.
26. Einterz, C. M., Hug, S. J., Lewis, J. W., and Kliger D. S. (1990) *Biochemistry 29*, 1485−1491.
27. Vought, B. W., Dukkipatti, A., Max, M., Knox, B. E., and Birge, R. R. (1999) *Biochemistry 38*, 11287−11297.
28. Shieh, T., Han, M., Sakmar, T. P., and Smith, S. O. (1997) *J. Mol. Biol. 269*, 373−384.
29. Birge, R. R. (1990) *Biochim. Biophys. Acta 1016*, 293−327.
30. Gärtner, W., and Towner, P. (1995) *Photochem. Photobiol. 62*, 1−16.
31. Bellingham, J., Wilkie, S. E., Morris, A. G., Bowmaker, J. K., and Hunt, D. M. (1997) *Eur. J. Biochem. 243*, 775−781.
32. Kitamoto, J., Sakamoto, K., Ozaki, K., Mishina, Y., and Arikawa, K. (1998) *J. Exp. Biol. 201*, 1255−1261.

BI991860Z